This article has been accepted for publication in IEEE Transactions on Biomedical Engineering. This is the author's version which has not been fully edited and content may change prior to final publication. Citation information: DOI 10.1109/TBME.2024.3513462

Preclinical Evaluation of a Wearable Wristband with Compressed-Sensing Based Photoplethysmography

Parvez Ahmmed, *Member, IEEE*, Emily Garceau, Tahmid Latif, *Member, IEEE*, Alec Brewer, James Dieffenderfer, Jose Manuel Valero-Sarmiento, Venkata Rajesh Pamula, *Member, IEEE*, Nick Van Helleputte, *Member, IEEE*, Chris Van Hoof, *Member, IEEE*, Marian Verhelst, *Fellow, IEEE*, and Alper Bozkurt, *Senior Member, IEEE*

***Abstract*— Photoplethysmography (PPG) has emerged as a highly convenient and non-invasive technique for assessing heart rate and its variability in wearable health monitoring devices. However, a drawback lies in the energy demand of PPG systems which consequently increases the average power consumption of wearable devices integrated with PPG sensors. In this paper, we present our efforts towards packaging a novel compressed-sensing (CS) based ultra-low power PPG application-specific integrated circuit (ASIC) into a wearable device and testing it through a preclinical human study. The system comprises a custom-designed ultra-low power PPG analog front-end circuit, integrated with a digital back-end to implement CS, and a commercial off-the-shelf microcontroller for Bluetooth Low Energy (BLE) based wireless data transfer. Two circular PCBs, a general-purpose main board, and a plugin board housing the ASIC interfacing components, fit into a wristband form factor. This modular architecture of the wristband platform allows for the incorporation of other environmental sensors for future correlated sensing studies between health and the environment. The PPG ASIC consumes 172 μW power to extract heart rate from the sparse PPG signal whereas the whole system consumes 1.66 mW power for continuous streaming of heart rate data over the BLE radio which can be further duty cycled. This work presents the first-ever demonstration of a wearable wristband with CS based PPG performed on a chip. The preclinical trial of the platform demonstrated its efficacy in assessing accurate heart rate in comparison to commercial PPG and electrocardiography systems.**

***Index Terms*— photoplethysmography, compressed sensing, sparse sampling, biomedical monitoring, Bluetooth Low Energy, wearable sensors, system validation, preclinical trials.**

Manuscript received May 30, 2024; revised October 31, 2024 and August XX, 2024; accepted August XX, 2024. Date of publication September XX, 2024; date of current version October 31, 2024. This work was supported by the National Science Foundation (NSF) under CCSS-1554367, IIS-2037328, IIS-1915599, ECCS-2231012, and ECC-1160483 grants. This paper was recommended by Associate Editor XXX. *(Corresponding author: Alper Bozkurt.)*

P. Ahmmed was with the Department of Electrical and Computer Engineering (ECE), NC State University, Raleigh, NC 27695-7911 USA. He is now with Advanced Micro Devices, Inc., Boxborough, MA 01719 USA (e-mail: p.ahmmed.bd@ieee.org).

E. Garceau, A. Brewer, and A. Bozkurt are with the Department of ECE, NC State University, Raleigh, NC 27695-7911 USA (e-mail: egarcea@ncsu.edu; ambrewe3@ncsu.edu; aybozkur@ncsu.edu).

T. Latif was with the Department of ECE, NC State University, Raleigh, NC 27695-7911 USA. He is now with the Wentworth Institute of Technology, Boston, MA 02115 USA (e-mail: latift@wit.edu).

J. Dieffenderfer was with the Department of ECE, NC State University, Raleigh, NC 27695-7911 USA. He is now with NIRSense Inc., Cary, NC 27518 USA (e-mail: james@nirsense.com).

J. M. Valero-Sarmiento was with the Department of ECE, NC State University, Raleigh, NC 27695-7911 USA. He is now with Apple Inc., Beaverton, OR 97006 USA (e-mail: josemanuel.valerosarmiento@gmail.com).

V. R. Pamula was with imec, Leuven 3001, Belgium. He is now with the Department of Electrical and Computer Engineering, University of Washington, Seattle, WA 98115 USA (e-mail: pamula@uw.edu).

N. Van Helleputte is with imec, Leuven 3001, Belgium (e-mail: nick.vanhelleputte@imec.be).

C. Van Hoof and M. Verhelst are with imec, Leuven 3001, Belgium, and also with the Department of Electrical Engineering (ESAT), Katholieke Universiteit (KU) Leuven, Leuven 3000, Belgium (e-mail: chris.vanhoof@imec.be; marian.verhelst@kuleuven.be).

Digital Object Identifier 10.1109/TBME.2024.XX

I. Introduction

GROWING social emphasis on personal health and well-being caused wearable physiological monitoring systems to gain tremendous popularity in recent years, particularly with their integration into consumer products such as smartwatches and fitness trackers. These wearable devices offer continuous monitoring of heart rate (HR) and its variability, crucial features that hold critical implications for assessing an individual's cardiovascular health status [1], [2]. Among the various methods available for HR assessment, photoplethysmography (PPG) stands out as a simple, compact, and noninvasive technique that utilizes on-skin optical sensing to detect changes in arterial blood volume within tissue [3], [4]. Unlike traditional HR monitoring methods, which often involve unpleasant body-attachments like adhesive electrodes for electrocardiography (ECG), wearable PPG devices offer a more user-friendly experience. These devices seamlessly integrate into users' daily routines and are minimally obtrusive, allowing for continuous monitoring without disrupting activities of daily life.

The commercially available fitness trackers and smartwatch devices with integrated biophotonic sensors have targeted user comfort to be one of the most important factors in the design consideration. While clinical systems are typically deployed on the clips placed on the finger, consumer products have been

Authorized licensed use limited to: N.C. State University Libraries - Acquisitions & Discovery S. Downloaded on December 18,2024 at 21:30:29 UTC from IEEE Xplore. Restrictions apply.
© 2024 IEEE. Personal use is permitted, but republication/redistribution requires IEEE permission. See https://www.ieee.org/publications/rights/index.html for more information.

This article has been accepted for publication in IEEE Transactions on Biomedical Engineering. This is the author's version which has not been fully edited and content may change prior to final publication. Citation information: DOI 10.1109/TBME.2024.3513462

TABLE I
COMPARISON OF THE KEY SPECIFICATIONS WITH THE STATE-OF-THE-ART AFES

Literature	**TBCAS'17 Our work [5]**	TBCAS'10 [6]	TBCAS'15 [7]	ESSCIRC'17 [8]	TBCAS'18 [9], [10]	ISSCC'21 [11]	TBCAS'22 [12]	SENSORS '24 [13]
Technology (µm)	**0.18**	1.50	0.18	0.18	0.18	0.18	0.04	COTS
Power supply (V)	**1.2**	5.0	1.8	-	3.3	1.2, 3.3	5, 1.1	2.8
Sampling rate (Hz)	**128 - 4**	100	165	160k	100, 40	2048	100 - 10	100
Noise RTI (pA_{rms})	**486**	-	2200	20.4	600	-	15.2	-
Noise BW (Hz)	**10**	-	6	10	10	20	5	16
LED control	√	×	√	√	√	√	√	√
Feature extraction	**HR, HRV**	SpO_2	-	-	HR	SpO_2	HR, SpO_2	HR/HRV, SpO_2
AFE power (µW)	**172**	400	216	13 - 25	27, 29	28	4.6 - 3.75	1330 - 165
LED power (µW)	**1200 - 43**	4400	1125 - 120	-	520 - 9	305	22.6 - 5.7	710 - 100

designed mostly to be worn on the wrist, especially with the growth in the smartwatch market. This placement also reduces motion artifacts, avoids interference with the motion of the hand and use of fingers, and allows for sufficient space to accommodate larger batteries, thereby reducing the frequency of charging. Quite a few similar wrist-worn physiological sensors in the literature [14], [15] use recently emerging commercial off-the-shelf (COTS) integrated circuits (ICs), such as AFE4400 (Texas Instruments, Dallas, TX, USA), for processing the raw PPG signal which consumes a substantial amount of power. Moreover, these systems often offer onboard wireless transmission capabilities to decrease wiring complexity, albeit at the expense of additional electrical power consumption [16]. Consequently, miniaturization of sensing devices and system-level power optimization are two of the ongoing challenges for system designers to ensure even more comfort and wearability [17].

PPG hardware consists of a light source (mostly light emitting diodes, LED), a light-sensing detector (mostly photodiodes, PD), a front-end circuit to amplify and/or filter the signal, and a digital control unit [18]. Among these components, the LED consumes the majority of the power, in the order of tens of mWs, to generate a sufficient amount of photons to interact with the hemodynamic system and bring heart rate modulated signals back to the detectors [19]. To address this power consumption issue, traditionally very low-duty-cycle pulses with a low sampling frequency are used [20], [21]. However, the sampling frequency and the duty cycle of the active pulses are limited by the Nyquist criterion and bandwidth of the circuit [22], [23].

Compressed sensing (CS) has been introduced to overcome the inherent redundancies of signal acquisition for applications where the signal of interest is sparse in any basis space [24]. This method promotes the use of random sampling instead of traditional uniform sampling by showing that the original waveform can be faithfully reconstructed from this minimally sampled signal, which has a lower effective sampling rate than the limits posed by the Nyquist-Shannon sampling theorem [25] and hence reduces the resource usage required for signal acquisition. Biological signals like PPG, which have a small number of non-zero (significant) components in the frequency domain (i.e. single frequency oscillation with minimal harmonic content), are suitable candidates for this optimized acquisition technique [26], [27].

In order to reduce the power consumption of the HR monitoring systems, we previously explored the CS approach and presented a PPG application-specific integrated circuit (ASIC) with a power consumption of 172 µW [5], [28]. This ASIC is capable of extracting the HR data from the compressed PPG signal with an effective sampling rate as low as 4 Hz. Table I displays the performance evaluations of some of the ultra-low-power PPG ASICs which are designed to consume less energy by using various alternative techniques like logarithmic amplifier [6], dynamic range enhancement [7], heart-beat locked loop (HBLL) [9], [10], [12], light-to-digital converter [8], [11], adaptive predictive sampling [13], etc. Among these techniques, HBLL is very similar to CS, as they both reduce the effective sampling rate. Although HBLL was not originally suitable for pulse oximetry (dual-wavelength PPG) as it did not generate any amplitude information, it was later improved in [12]. However, both of these works are vulnerable to motion artifacts as these techniques heavily depend on transient features. On the other hand, CS, along with some frequency-domain post-processing steps similar to [29], [30], can be more suitable for practical use cases. Moreover, it is important to note that all these reported specifications are based on benchtop evaluations, primarily conducted on the finger, which is a favorable setup for low power consumption. Further evaluation within wearable form factors and human testing would provide a more fair and practical benchmark between these ASICs.

With this goal, we have packaged the CS PPG ASIC into a miniaturized wearable form factor in order to evaluate its usability to track HR on the wrist [31]. The goal of the work presented here was the preclinical evaluation of the wearable PPG wristbands through an Institutional Review Board (IRB) approved human study to assess the system's efficacy. This study was performed under the United States National Science Foundation (NSF) Engineering Research Center (ERC) for Advanced Self-powered Systems of Integrated Sensors and Technologies (ASSIST) at NC State University, Raleigh, NC, USA, in collaboration with Interuniversity Microelectronics Centre (imec) and Katholieke Universiteit (KU) Leuven in Belgium. ASSIST designs, manufactures, and evaluates low-power wearable sensors for correlated sensing of health and exposure [32]. Section II describes the hardware and software

Authorized licensed use limited to: N.C. State University Libraries - Acquisitions & Discovery S. Downloaded on December 18,2024 at 21:30:29 UTC from IEEE Xplore. Restrictions apply.
© 2024 IEEE. Personal use is permitted, but republication/redistribution requires IEEE permission. See https://www.ieee.org/publications/rights/index.html for more information.

This article has been accepted for publication in IEEE Transactions on Biomedical Engineering. This is the author's version which has not been fully edited and content may change prior to final publication. Citation information: DOI 10.1109/TBME.2024.3513462

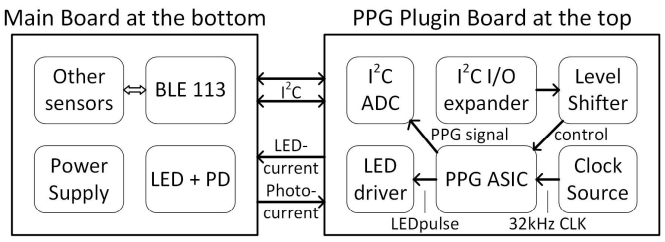

Fig. 1. Diagram of the PPG readout circuit showing connectivity among the major blocks of the modular system [31].

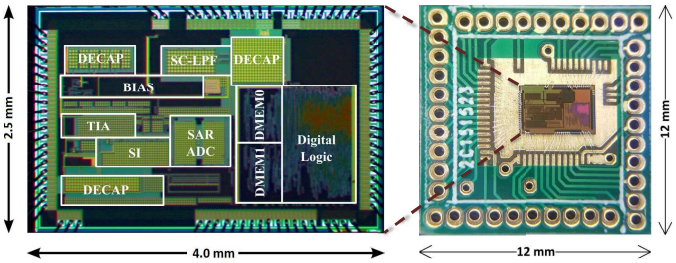

Fig. 2. Wirebonding of the ASIC on the custom PCB.

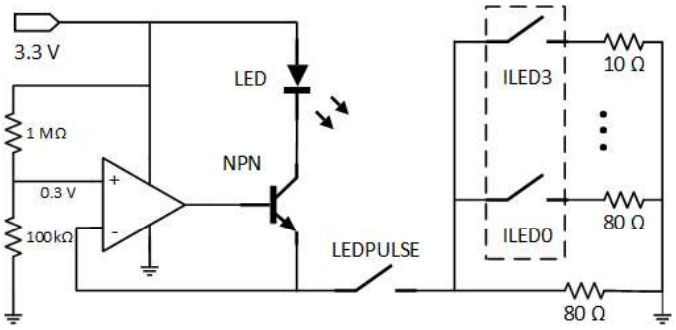

Fig. 3. Schematic of the LED driver circuit which is designed to drive up to 60 mA current with a resolution of 3.75 mA [31]. The opamp sets a fixed voltage at the emitter of the transistor (NPN BJT), followed by an electronic switch to control the duty cycle of the LED pulses and a digitally programmable resistor bank to control the I_{LED}.

interfacing of the CS PPG ASIC with ASSIST's modular system and Section III presents the in vivo experimental protocol and the methods for extracting HR from the recorded signals. The comparison of this system with a commercial HR monitoring platform in stationary and physically active subjects is demonstrated in Section IV. CS stands out as a promising ultra-low power PPG technique, especially with this presented study demonstrating the wearable form factor and its practical use on the wrist.

II. System Design and Implementation

We have designed the wearable wristband platform in this work following ASSIST's flexible architecture (Fig. 1) that consists of a main board for central processing and plugin boards for additional features. This allows for the use of the same main board with various ASSIST plugin boards housing energy harvesters (e.g. solar or thermoelectric) or other sensor subsystems, such as inertial measurement units, ultra-low-power ozone sensors, or volatile-organic-compound sensors to assess air quality, for future correlated studies.

A. Compressed Sensing PPG ASIC

The designed PPG ASIC has three major blocks: 1) an analog front end (AFE) to process the photocurrent from the PD; 2) a successive-approximation-register (SAR) analog-to-digital converter (ADC) to digitize the analog signal; and 3) a digital back end (DBE) capable of implementing CS with a selectable compression ratio (CR) of 8x, 10x, and 30x with the help of a 32 kHz clock signal provided externally. As the ASIC design is detailed in [5], only the features relevant to system interfacing are revisited here.

The AFE is comprised of a transimpedance amplifier (TIA), a digital-to-analog converter (DAC), and a switched integrator (SI). The current DAC cancels out a programmable portion of the DC component of the photocurrent at the input of TIA in order to avoid saturating the readout circuit and to increase the dynamic range. The TIA is implemented using a Miller-compensated operational transconductace amplifier (OTA) with resistive feedback (R_f). While connecting to a PD, stability issues can arise due to the reverse bias junction capacitance of the PD (C_p). Hence, a compensation capacitor (C_f) is added in parallel to R_f to introduce an LHP zero, thereby improving the stability margin of the TIA. Both the feedback resistor and capacitor can be tuned to adapt to different operating conditions, as the PPG signal varies widely depending on factors such as skin tone and location on the body.

The input capacitance from the PD (C_p) coupled with relatively lower values of feedback capacitor (C_f) of the TIA causes peaking in the noise transfer function, which necessitates the addition of a low-pass filter. This is particularly important in pulsed PPG acquisition systems, to include the noise limiting filter before the signal is sampled [21]. Hence, the SI is included as the second stage in the readout circuit which also adds extra gain to the signal path tunable by programming the feedback capacitor (C_{int}).

B. Interfacing the PPG ASIC

The 4.0 × 2.5 mm^2 bare die of the ASIC has 84 bond pads in total. The use of a standard plastic-leaded chip carrier (PLCC) to attach the ASIC would consume an area of 35.9 × 35.9 mm^2 and could be challenging to accommodate within a wrist-worn form factor. With the aim of miniaturization, a custom 12 × 12 mm^2 printed circuit board (PCB) is designed to host the bare die instead of the standard PLCC package (Fig. 2) to access only the necessary connections, which is sufficient for system operation. The bare die of the ASIC is attached to the ground plane of this breakout board with silver conductive epoxy (8331, MG Chemicals Ltd., Surrey, BC, Canada) and heat-cured at 65 °C for 20 minutes. The chip is, then, bonded with an ultrasonic/thermosonic wedge-wedge wirebonder (7476E, WESTBOND Inc., Anaheim, CA, USA) using aluminum wire of 1 µm diameter.

The various programmable components of the ASIC mentioned in the previous subsection need to be controlled by the

Authorized licensed use limited to: N.C. State University Libraries - Acquisitions & Discovery S. Downloaded on December 18,2024 at 21:30:29 UTC from IEEE Xplore. Restrictions apply.
© 2024 IEEE. Personal use is permitted, but republication/redistribution requires IEEE permission. See https://www.ieee.org/publications/rights/index.html for more information.

This article has been accepted for publication in IEEE Transactions on Biomedical Engineering. This is the author's version which has not been fully edited and content may change prior to final publication. Citation information: DOI 10.1109/TBME.2024.3513462

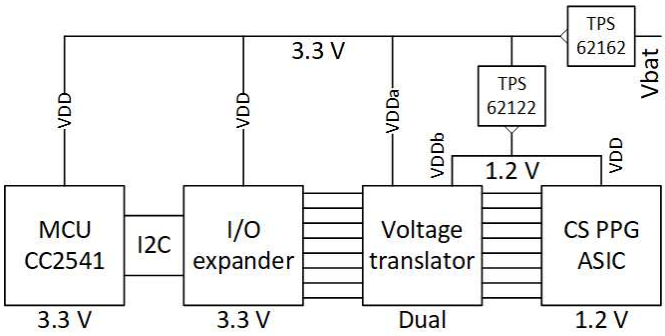

Fig. 4. Schematic of IO conditioning circuitry along with supply voltage regulation topology [31].

central system. It ends up requiring 16 digital input-output (IO) pins for adjusting the gain and bandwidth of the amplifying and filtering stages of the AFE, the PD bias cancellation current (I_{DAC}), the CR of random sampling, etc. Moreover, the onboard LED driver (Fig. 3) has a 4-bit analog switch (TS3A4751, Texas Instruments) which is used to control the LED brightness by changing the current (I_{LED}).

In order to let the microcontroller access all these connections with the limited number of GPIO pins, we used commercially available I^2C-based IO expanders (PCF8574 & PCF8575, Texas Instruments). Unlike the rest of the system comprised of commercial integrated circuits using 3.3 V power supply, the ASIC is designed to operate at 1.8 V supply voltage to keep the power consumption low. To exchange the voltage levels, we have used several 8-bit voltage translators (NLSV8T244, ON Semiconductor, Denver, CO, USA) placed between the IO expanders and the ASIC (Fig. 4). The 32 kHz clock signal required for the ASIC could also be provided by the microcontroller through one of the voltage translator lines, but to reduce noise and jitter, the clock signal is generated directly from a 555 timer IC (LMC555, Texas Instruments).

There were three ways to digitally record the analog PPG signal: 1) using the internal 12-bit SAR ADC which would need more IO expanders and voltage translators and hence draw additional power (estimated to be 27 µW); 2) using the ADC peripheral of the microcontroller which usually consumes even more power (1200 µW in our case); or 3) using a low-power external ADC IC which is fast enough to respond and sample within the narrow pulse width of the switched output. Moreover, while experimenting with the microcontroller's peripheral ADC, we noticed that its input impedance is lower, and hence the sampling current drawn by the ADC caused PPG signal deformations. As a result, we used an ultra-fast ADC IC (ADS7142, Texas Instruments) which can be operated through I^2C commands in single-shot mode and consume approximately 27 µW according to its datasheet.

C. The Modular PCB Approach

All the aforementioned components along with the ASIC breakout board are soldered into a circular PCB of 3 mm diameter. For modularity, this PCB (plugin board) is plugged onto another general-purpose PCB (main board) of the same size (Fig. 5a) that houses the system-on-a-chip (SoC). As

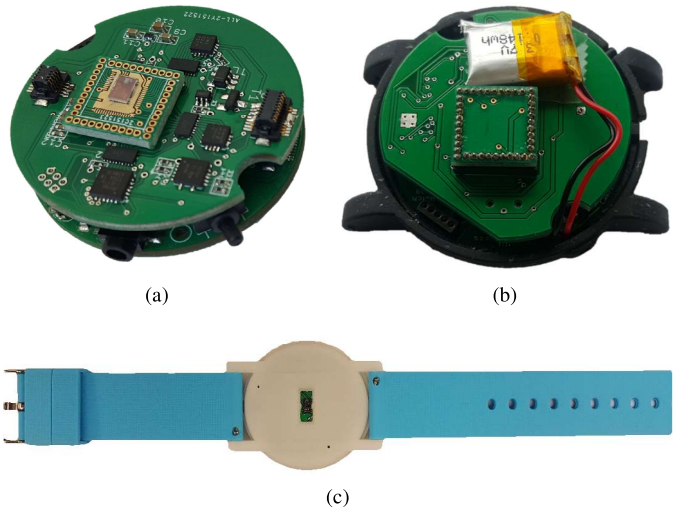

Fig. 5. (a) Modular System design where the main (bottom) board houses the microcontroller and the power supply block, and the plugin board houses the wire-bonded PPG ASIC and the other interfacing ICs. (b) The actual placement of the PCBs in the 3D-printed case. (c) The back side of the wristband shows the optical sensor [31].

mentioned earlier, this modular architecture is intended for future validation of these sensors in the clinics, for example, to correlate the vital health signs with the air quality measures [32].

The main board houses a Bluetooth Low Energy (BLE) radio transceiver (Bluegiga BLE113, Silicon Laboratories, Inc., Austin, TX, USA) controlled by an SoC (CC2541, Texas Instruments). This board also contains other COTS ICs including memory, ADC, etc. to accommodate the broader range of requirements for various plugin sensor boards. The system is powered by a 150 mW rechargeable Li-ion polymer battery which is regulated to 3.3 V by a switching regulator or Buck converter (TPS62162, Texas Instruments). The voltage regulation from 3.3 V to 1.8 V for the PPG ASIC is performed by another switching regulator (TPS62122, Texas Instruments) in the plugin board (Fig. 4).

All components required for interfacing the PPG ASIC are placed in the plugin board (Fig. 1) except the LED and PD which are placed underneath the main board, on the opposite and tissue side, to access the skin through a rectangular window in the 3D printed casing (Fig. 5c). One of the major challenges in getting good-quality PPG signals is ensuring consistent skin contact. For this, we have used a small castellated board to solder the light source-detector couple, so that it protrudes out from the casing slightly providing a much secure contact. The current system uses a multi-LED and single-PD package (SFH7050 BioMon Sensor, OSRAM Opto Semiconductors GmbH, Regensburg, Germany) in order to allow for switching wavelengths. Previously, we had used the red (660 nm) LED on this package for evaluation purposes following the general trend of routine clinical applications [5]. In this study, we explored the quality of the PPG signal using the green (525 nm) LED and observed that it produces stronger PPG pulses at this location. This wavelength is also less prone to bias sensitivity resulting in better motion artifact

Authorized licensed use limited to: N.C. State University Libraries - Acquisitions & Discovery S. Downloaded on December 18,2024 at 21:30:29 UTC from IEEE Xplore. Restrictions apply.
© 2024 IEEE. Personal use is permitted, but republication/redistribution requires IEEE permission. See https://www.ieee.org/publications/rights/index.html for more information.

This article has been accepted for publication in IEEE Transactions on Biomedical Engineering. This is the author's version which has not been fully edited and content may change prior to final publication. Citation information: DOI 10.1109/TBME.2024.3513462

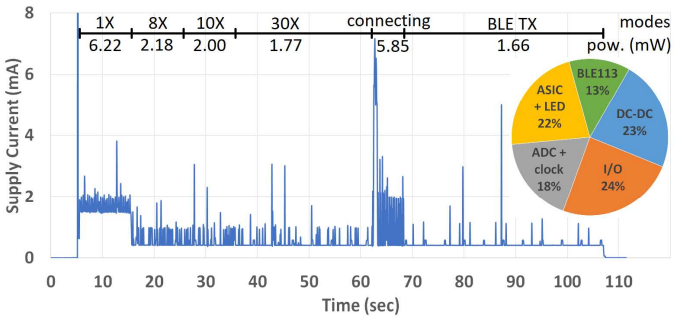

Fig. 6. Transient plot of supply current at 3.7 V input and average power consumption at different modes of operation [31]. The distribution of power consumption among the different components on the boards during the transmission phase at CR = 30x is shown in the pie chart.

TABLE II
PARTICIPANT DEMOGRAPHICS OF 21 SUBJECTS (13 MALE, 8 FEMALE)

Parameter	mean	SD	minimum	maximum
Age (years)	27.00	9.60	19.00	60.00
Height (cm)	173.09	9.60	152.40	185.42
Mass (kg)	67.25	15.18	43.00	102.06
BMI (kg/m^2)	22.26	3.99	16.80	35.24

rejection [33].

After the wristband assembly was completed, the overall power consumption of the system was measured using a source meter (Model 2450, Keithley Instruments, Cleveland, OH, USA). For demonstration purposes, the sampling mode has been switched between different CR modes (including uniform sampling). The total power consumption of the system including BLE data transfer is measured to be 1.66 mA (Fig. 6), which is mostly due to wireless transmission, and can be further reduced with proper duty cycling of the BLE packages depending on the application.

III. EXPERIMENTAL METHODS

Before the wrist, the first measurements were taken on the fingers to evaluate the system against the earlier finger-based assessment [5]. We placed the circular PCB on the index finger of the subject and ensured a tight enough skin coupling of the BioMon sensor to acquire a strong PPG response. We observed that the single-ended design of the TIA makes the output bias level relatively more sensitive to the applied pressure or motion artifacts. To overcome this, we implemented a closed-loop adaptive control in the embedded software. This protects the PPG signal from going into saturation by adjusting the I_{DAC} dynamically. Whenever the sampled signal goes within 100 mV of the supply rails, the microcontroller changes the I_{DAC} setting to adjust the DC component of the input photocurrent. The voltage step appearing in the raw PPG data is removed from the signal during post-processing by canceling out any abrupt voltage shifts.

After this initial experimentation on the finger, we performed the preclinical evaluation and validation of the CS PPG wristband on 21 subjects (demographics are tabulated in Table II) in two phases: 15 subjects participated in stationary

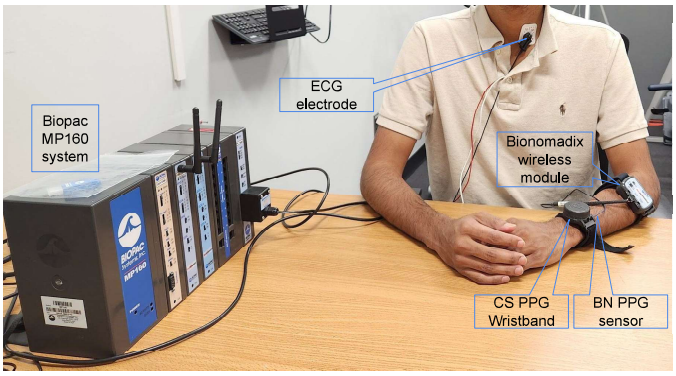

Fig. 7. In vivo experimental setup showing the CS and BIOPAC devices.

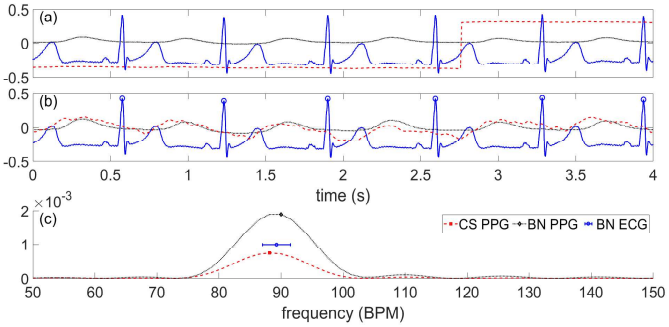

Fig. 8. (a) Transient plot of the uniformly-sampled raw PPG signal recorded from the three devices. (b) The shift in bias levels is removed from the CS PPG signal and peak detection is performed on the BN ECG signal. (c) The frequency domain plots of the PPG signals showing the detected HR values in comparison with the mean±SD of the HR values from the ECG signal.

studies and 6 subjects performed physical activities during data collection. The experimental procedure was approved by the IRB at NC State University under protocol Number 12418. For validation and comparison, we used two other commercial systems from BIOPAC Systems, Inc., Goleta, CA, USA: BioNomadix (BN) wireless PPG (BN-PPGED) and wired ECG (ECG100C) modules connected to a benchtop system (MP160 Data Acquisition System). In the case of physical activities, the BN wireless ECG module (ECG2R) is used. HR from this commercial ECG system was used as the gold standard. CS PPG recordings were used to benchmark against the commercial PPG system. During the experiments, the subjects sat on a chair wearing the CS PPG wristband on the left hand along with the BN PPG sensor underneath the strap of the wristband to ensure similar location and contact pressure for both PPG sensors (Fig. 7). The BN ECG system was connected to three standard wet-gel electrodes (Red Dot™ 2560, 3M, Saint Paul, MN, USA) attached to the chest. Then, we collected four sessions of data for the four CR configurations of the CS PPG wristband while the subjects were resting their arm on the table.

All the collected data is first passed through a Hampel filter from Matlab (Mathworks, Natick, MA, USA) to remove outliers in the raw data [34]. The CS PPG signal is then adjusted for any large bias shifts originating from the change in I_{DAC} current setting (Fig. 8b). To realize CS *in silico*, the

Authorized licensed use limited to: N.C. State University Libraries - Acquisitions & Discovery S. Downloaded on December 18,2024 at 21:30:29 UTC from IEEE Xplore. Restrictions apply.
© 2024 IEEE. Personal use is permitted, but republication/redistribution requires IEEE permission. See https://www.ieee.org/publications/rights/index.html for more information.

This article has been accepted for publication in IEEE Transactions on Biomedical Engineering. This is the author's version which has not been fully edited and content may change prior to final publication. Citation information: DOI 10.1109/TBME.2024.3513462

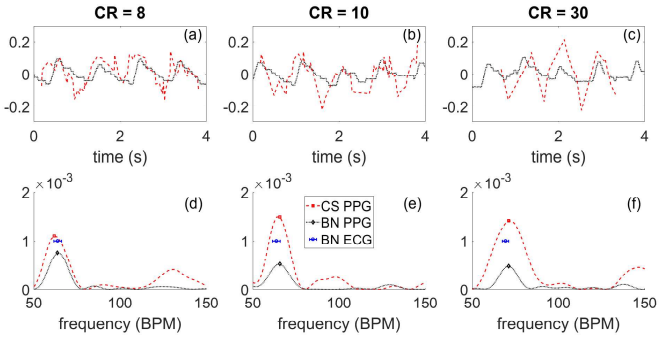

Fig. 9. (a-c) Transient plot of the randomly-sampled PPG signal recorded from CS wristband using different CR along with the BN PPG signal. ECG signal is omitted for clarity. (d-f) The Lomb-Scargle periodogram of the CS PPG data and the regular periodogram of the BN PPG data showing the detected HR values in comparison with the mean±SD of the HR values from the ECG signal.

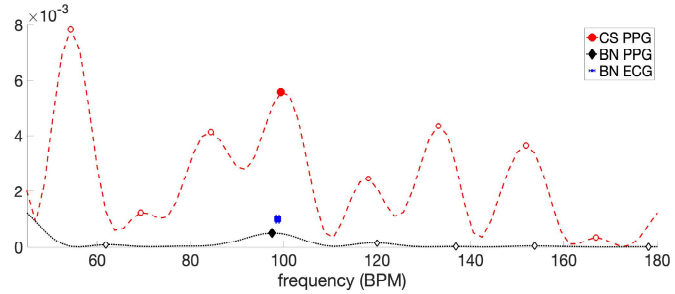

Fig. 10. The Lomb-Scargle periodogram of the CS PPG data and the regular periodogram of the BN PPG data showing the selection of HR peak from motion-corrupted signal along with the average HR value from the ECG signal.

ASIC generates a pseudo-random sequence of timing pulses that repeats every four seconds. This pulse train activates the LEDs and the AFE simultaneously to realize the random sampling. Hence, all the signals were sliced into 4-second windows before extracting any HR information.

Theoretically, it is possible to reconstruct the PPG signal from the CS data, but as we are interested in the extraction of HR, the Lomb-Scargle periodogram (LSP) method [35], [36] is applied to each 4-second segment to generate the power spectral density (PSD) of the PPG signal (see Fig. 9). The linear trend was removed from individual data segments before applying the LSP algorithm as elaborated in the Appendix.

The uniformly sampled data from both the CS and BN devices were also split into the same 4-second windows for consistency. The PPG data were treated with fast Fourier transform (FFT) to extract the HR (Fig. 8c). For the BN ECG signal, the instantaneous HR was first extracted from the inverse of the peak-to-peak interval and then averaged over the 4-second windows.

Within the context of this paper, since the main focus is to demonstrate miniaturization and verify the effectiveness of CS in the power reduction of PPG, data collection from stationary subjects is primarily used for system validation. Physical exercise and activities of daily life affect the quality of PPG acquisition by introducing undesired signal artifacts. Although there are several time-domain and frequency-domain

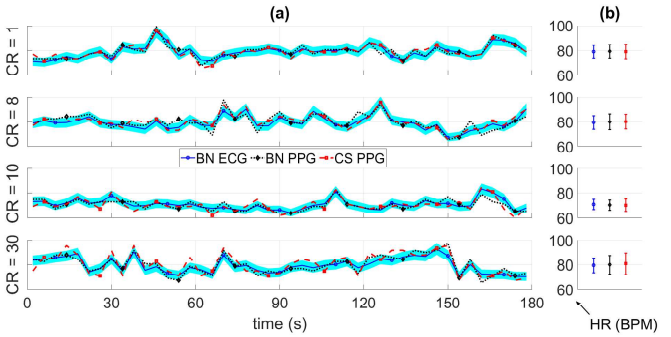

Fig. 11. (a) Example of transient plots comparing the HR values in BPM (using the 4-second window) obtained from all three devices. The blue patch denotes the 5% tolerance range around the gold-standard estimation. (b) The mean±SD of the HR values.

techniques for removing motion artifacts for biosignals, they are mostly applicable to uniformly sampled data [37]. Among these, a few techniques that rely on sparse spectral methods have the potential to be used with randomly sampled data as CS also relies on sparsity of the signal. Hence, PPG performance during varying levels of motion and the use of an appropriate motion artifact rejection technique necessitates a more comprehensive and future study [38].

However, we have collected preliminary proof-of-concept data during a walking activity (0.67 m s^{-1} speed on a treadmill) from six additional subjects to show how a sparse spectral technique (FOCUSS [29], TROIKA [30], etc.) can be adopted for CS PPG data. As an initial attempt, we focused on TROIKA which has three essential parts: signal decomposition for denoising, sparse signal reconstruction for high-resolution spectrum estimation, and spectral peak tracking with verification [30]. In our current implementation, LSP works as a weak alternative to the first two parts, as LSP does not produce sufficient spectral resolution for motion artifact removal. Hence, both the CS and BN PPG data affected by motion artifacts were treated with only one extra post-processing step similar to the last step from TROIKA after extracting the LSP periodogram from each 4-second window.

The TROIKA framework divides spectral peak tracking into three main components: initialization, peak selection, and verification. The tracker is initialized with the HR values obtained by identifying the frequency with the highest PSD same as before. For each subsequent 4-second window of exercise data, we identified all peaks in the Lomb-Scargle periodogram within a frequency range of ±0.25 Hz (±15 BPM) of the previous window's identified HR values and the appropriate one was selected according to the framework (Fig. 10). Finally, the HR values were verified with a regularization-based method to compensate for large changes.

IV. Results from Validation Experiments

The HR values from both the PPG signals (recorded by CS and BN devices) were compared with those from the gold-standard ECG signal. Fig. 11 shows the example plots of the HR values from one subject at different CR configurations. The HR values from both the PPG signals mostly followed the HR values from the gold-standard ECG within a 5% tolerance

Authorized licensed use limited to: N.C. State University Libraries - Acquisitions & Discovery S. Downloaded on December 18,2024 at 21:30:29 UTC from IEEE Xplore. Restrictions apply.
© 2024 IEEE. Personal use is permitted, but republication/redistribution requires IEEE permission. See https://www.ieee.org/publications/rights/index.html for more information.

This article has been accepted for publication in IEEE Transactions on Biomedical Engineering. This is the author's version which has not been fully edited and content may change prior to final publication. Citation information: DOI 10.1109/TBME.2024.3513462

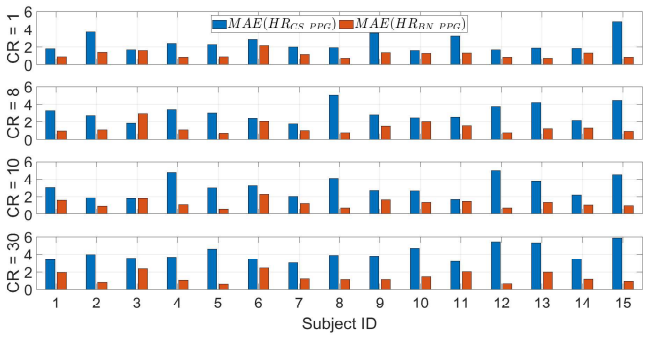

Fig. 12. Mean absolute error in HR estimation in BPM obtained from the PPG devices with respect to the gold-standard ECG device.

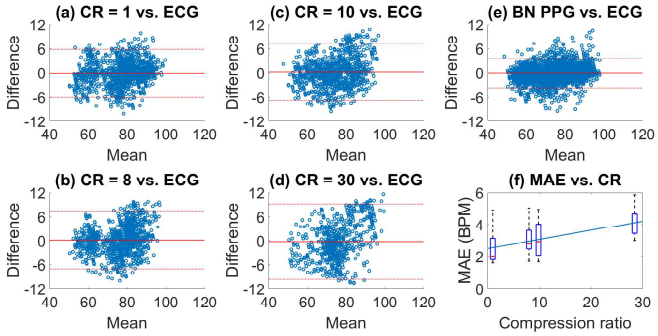

Fig. 13. Bland-Altman plots comparing the HR values from (a-d) CS PPG with different CRs and (e) BN PPG in comparison with that from the gold-standard ECG. (f) The effect of compression ratio on the HR estimation errors in the case of CS PPG.

range [39]. The mean±SD of the HR values also show a good agreement.

Fig. 12 shows the mean absolute error (MAE) of the HR from CS PPG and BN PPG compared to that from the BN ECG. The average MAE obtained from the CS PPG device is 1.95, 2.6, 2.8, and 3.94 BPM at compression ratios of 1, 8, 10, and 30, respectively. Although CS PPG showed higher MAE than the commercial BN PPG (1.3 BPM, on average); it should be noted that the BN device uses a much higher sampling rate (2000 Hz) and more energy resources for its circuits and the LED drivers.

The Bland-Altman plots [40] in Fig. 13 show the mean±SD of the error values in different CR configurations. It is evident again that, except CR=30, all the other CR configurations resulted in a similar range of errors. One-way ANOVA test and linear regression on the MAE values show a significant correlation ($p < 10^{-4}$) between the MAE and CR configurations (Fig. 13f). Medium-level compression resulted in minimal error in HR estimation compared to commercial PPG systems and the gold-standard ECG system.

While we present the power consumed by the AFE, DBE, and LED driver along with MAE of HR estimation obtained through in vivo human subject testing, it is relatively challenging to benchmark these with other work in the literature since all these systems were evaluated under different in vivo experimental conditions. The following factors are not standard between these studies cited in Table I: 1) measurement location on the body, 2) presence and intensity of

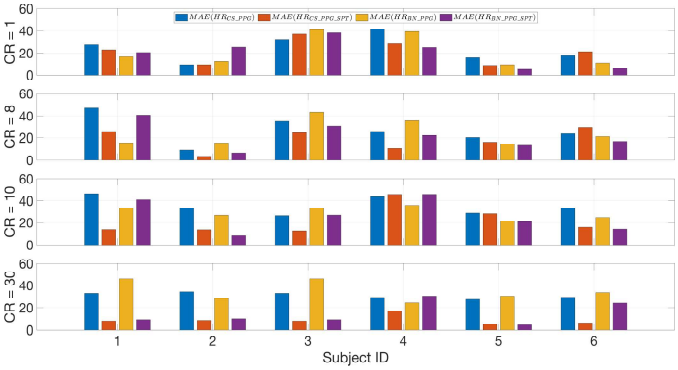

Fig. 14. Mean absolute error in HR estimation in BPM obtained from the PPG devices with respect to the gold-standard ECG device during physical activity.

physical activity and hence the motion artifacts during data acquisition, 3) body-mass index and skin tone of the subjects, and 4) system hardware including a novel ASIC or using only COTS integrated circuits or components. PPG measurement from the fingers generally generates better results compared to the wrist (e.g., [12]). Among the presented work in Table I, [13] had a particular focus on developing an application-specific signal processing method using adaptive predictive sampling incorporated into COTS component based circuit design, thereby demonstrating superior results despite motion artifacts.

Our device produced promising results on the wrist of stationary subjects where the improvement for motion artifacts requires a special focus on new signal processing methods that can handle compressed-sensing signals. This is kept beyond the scope of this presented study and as a future work. However, we still evaluated the effect of the motion artifacts and implemented straightforward solutions to reduce the impact on the signal quality.

The MAE is expected to deteriorate in the presence of motion artifacts from physical activities. Fig. 14 shows the improvement of HR estimation, thanks to the application of spectral peak tracking from the TROIKA framework. As demonstrated in [30], the peak tracking step alone cannot fully improve the estimation error. Overall, TROIKA improved the MAE from 28.7 BPM to 17.3 BPM which is actually better than the MAE obtained from the commercial BN device (improved from 27.4 BPM to 20.0 BPM). Hence, we speculate that the real cause of the MAE is not the CS topology itself but the need for motion artifact reduction by implementing effective signal processing tools, similar to the one demonstrated by [13] for non-compressed PPG signals.

While the spectral peak tracking and use of TROIKA framework did improve the accuracy under motion artifacts, there is a considerable amount of room for further improvements in the signal processing domain. This warrants a separate study and publication to develop proper motion artifact techniques specific to CS PPG signals. We recommend that the first research problem to solve in the future would be to develop an alternative or improvement of the LSP algorithm that can generate high-resolution spectral information from randomly sampled data. This would also necessitate the adoption of

Authorized licensed use limited to: N.C. State University Libraries - Acquisitions & Discovery S. Downloaded on December 18,2024 at 21:30:29 UTC from IEEE Xplore. Restrictions apply.
© 2024 IEEE. Personal use is permitted, but republication/redistribution requires IEEE permission. See https://www.ieee.org/publications/rights/index.html for more information.

This article has been accepted for publication in IEEE Transactions on Biomedical Engineering. This is the author's version which has not been fully edited and content may change prior to final publication. Citation information: DOI 10.1109/TBME.2024.3513462

denoising techniques for CS data. Once a reliable periodogram is obtained, the existing peak tracking algorithms can be used to enhance the temporal tracking of HR. Lastly, the improved algorithm can be implemented in ASIC as a part of the feature extraction unit.

V. Conclusion

This paper demonstrates the first-ever integration and evaluation of a novel compressed-sensing based ultra-low power photoplethysmography ASIC into a wearable wristband platform. The ASIC provides an analog front-end circuit and a digital back-end for low-power PPG signal acquisition. The system miniaturization effort towards a wearable form factor is achieved along with no compromise in the performance of the ASIC. The ASIC power consumption is as low as 172 µW where the overall system consumed 1.66 mW. Most of this was due to wireless Bluetooth transmission and can be further reduced in the next iteration of the ASIC design by replacing the COTS SoC with a more application-specific SoC as well as optimizing the ASIC for the targeted application. Finally, we evaluated the performance of the wristband with in vivo experiments through an IRB-approved preclinical trial on a total of 21 subjects and compared the accuracy of heart rate extraction with a commercially available PPG system. With respect to the gold-standard ECG system, medium-level compression resulted in minimal error of HR estimation in stationary subjects compared to the commercial PPG system. The results from this study confirm that compressed sampling is a promising method to reduce the energy requirements of PPG systems with a reasonable trade-off for measurement accuracy on stationary subjects. The results also warrant the need for the development of novel signal processing techniques to remove motion artifacts from compressed sensing PPG signals.

Appendix

Let $x(t_j),\ j = 1, 2, \ldots, M$ be the CS PPG samples where M is the number of pseudo-random samples collected at the timestamps t_j within a 4-second window. LSP estimates the PSD (P_X) of $x(t_j)$ as a function of angular frequency (ω_i) using (1) and the frequency at the maxima of PSD gives the value of HR.

$$P_X(\omega_i) = \frac{\left(\sum_{j=1}^{M} x_0(t_j)\ c_{ij}\right)^2}{\sum_{j=1}^{M} c_{ij}^2} + \frac{\left(\sum_{j=1}^{M} x_0(t_j)\ s_{ij}\right)^2}{\sum_{j=1}^{M} s_{ij}^2} \quad (1)$$

where

$$\begin{aligned} x_0(t_j) &= x(t_j) - \overline{x}; \\ c_{ij} &= \cos\left(\omega_i(t_j - \tau_i)\right); \\ s_{ij} &= \sin\left(\omega_i(t_j - \tau_i)\right). \end{aligned}$$

As the values of ω_i and t_j are already known *a priori* from the frequency range of interest and ASIC's sampling instants respectively, the values of coefficients, c_{ij} and s_{ij}, can be pre-calculated using

$$\tau_i = \frac{1}{2\pi} \tan^{-1}\left(\frac{\sum_{j=1}^{M} \sin\left(2\omega_i t_j\right)}{\sum_{j=1}^{M} \cos\left(2\omega_i t_j\right)}\right)$$

This simplification (faster compared to the truly random case where the sampling instants are not known beforehand [41]) paves the way to implementing the LSP algorithm in the firmware making the platform ready for real-time HR extraction in the future.

Acknowledgment

The authors would like to thank Steve Lipa for wirebonding the ASIC on the custom PCB, Dr. Bongmook Lee for coordinating the preclinical human study, and the human subjects for participating in the validation experiments.

References

[1] X.-F. Teng *et al.*, "Wearable medical systems for p-health," *IEEE Reviews in Biomedical Engineering (RBME)*, vol. 1, pp. 62–74, Dec. 2008.

[2] A. Hughes *et al.*, "Wearable devices in cardiovascular medicine," *Circulation Research*, vol. 132, no. 5, pp. 652–670, 2023.

[3] J. Allen, "Photoplethysmography and its application in clinical physiological measurement," *Physiological Measurement*, vol. 28, no. 3, R1–R39, Feb. 2007.

[4] C. Brüser *et al.*, "Ambient and unobtrusive cardiorespiratory monitoring techniques," *IEEE Reviews in Biomedical Engineering (RBME)*, vol. 8, pp. 30–43, Mar. 2015.

[5] V. R. Pamula *et al.*, "A 172 µW compressively sampled photoplethysmographic (PPG) readout ASIC with heart rate estimation directly from compressively sampled data," *IEEE Transaction on Biomedical Circuits and Systems (TBCAS)*, vol. 11, no. 3, pp. 487–496, Jun. 2017.

[6] M. Tavakoli, L. Turicchia, and R. Sarpeshkar, "An ultra-low-power pulse oximeter implemented with an energy-efficient transimpedance amplifier," *IEEE Transactions on Biomedical Circuits and Systems (TBCAS)*, vol. 4, no. 1, pp. 27–38, Feb. 2010.

[7] E. S. Winokur, T. O'Dwyer, and C. G. Sodini, "A low-power, dual-wavelength photoplethysmogram (PPG) SoC with static and time-varying interferer removal," *IEEE Transactions on Biomedical Circuits and Systems (TBCAS)*, vol. 9, no. 4, pp. 581–589, Aug. 2015.

[8] H.-G. Kim and D.-W. Jee, "A <25 µW cmos monolithic photoplethysmographic sensor with distributed 1b delta-sigma light-to-digital convertor," in *43rd IEEE European Solid State Circuits Conference (ESSCIRC)*, 2017, pp. 55–58.

[9] D. H. Jang and S. Cho, "A 43.4 µW photoplethysmogram-based heart-rate sensor using heart-beat-locked loop," in *IEEE International Solid-State Circuits Conference (ISSCC)*, Feb. 2018, pp. 474–476.

[10] J. Lee *et al.*, "A low-power photoplethysmogram-based heart rate sensor using heartbeat locked loop," *IEEE Transactions on Biomedical Circuits and Systems*, vol. 12, no. 6, pp. 1220–1229, 2018.

[11] Q. Lin *et al.*, "A 28µW 134dB DR 2nd-order noise-shaping slope light-to-digital converter for chest PPG monitoring," in *IEEE International Solid- State Circuits Conference (ISSCC)*, vol. 64, 2021, pp. 390–392.

[12] S. F. Alamouti *et al.*, "A sparse sampling sensor front-end IC for low power continuous SpO_2 & HR monitoring," *IEEE Transactions on Biomedical Circuits and Systems*, vol. 16, no. 6, pp. 997–1007, 2022.

[13] Z. Ebrahimi and B. Gosselin, "An ultralow-power PPG sensor with adaptive predictive sampling," *IEEE Sensors Journal*, vol. 24, no. 9, pp. 14 137–14 150, 2024.

[14] S. S. Thomas *et al.*, "Demonstration abstract: BioWatch – a wrist watch based physiological signal acquisition system," in *Proceedings of the 13th International Symposium on Information Processing in Sensor Networks*, Apr. 2014, pp. 349–350.

[15] T. Sheng *et al.*, "The design of wearable sleep apnea monitoring wrist watch," in *IEEE 19th International Conference on e-Health Networking, Application and Services (Healthcom)*, Oct. 2017, pp. 1–6.

Authorized licensed use limited to: N.C. State University Libraries - Acquisitions & Discovery S. Downloaded on December 18,2024 at 21:30:29 UTC from IEEE Xplore. Restrictions apply.
© 2024 IEEE. Personal use is permitted, but republication/redistribution requires IEEE permission. See https://www.ieee.org/publications/rights/index.html for more information.

This article has been accepted for publication in IEEE Transactions on Biomedical Engineering. This is the author's version which has not been fully edited and content may change prior to final publication. Citation information: DOI 10.1109/TBME.2024.3513462

[16] A. Pantelopoulos and N. G. Bourbakis, "A survey on wearable sensor-based systems for health monitoring and prognosis," *IEEE Transactions on Systems, Man, and Cybernetics, Part C (Applications and Reviews)*, vol. 40, no. 1, pp. 1–12, Oct. 2010.

[17] D. Dias and J. Paulo Silva Cunha, "Wearable health devices–vital sign monitoring, systems and technologies," *Sensors (Basel)*, vol. 18, no. 8, Jul. 2018, Article no. 2414.

[18] Q. Lin *et al.*, "Photoplethysmography (PPG) sensor circuit design techniques," in *IEEE Custom Integrated Circuits Conference (CICC)*, 2022.

[19] Z. Ebrahimi and B. Gosselin, "Ultralow-power photoplethysmography (PPG) sensors: A methodological review," *IEEE Sensors Journal*, vol. 23, no. 15, pp. 16 467–16 480, 2023.

[20] A. K. Y. Wong *et al.*, "A low-power CMOS front-end for photoplethysmographic signal acquisition with robust DC photocurrent rejection," *IEEE Transactions on Biomedical Circuits and Systems (TBCAS)*, vol. 2, no. 4, pp. 280–288, Dec. 2008.

[21] K. N. Glaros and E. M. Drakakis, "A sub-mW fully-integrated pulse oximeter front-end," *IEEE Transactions on Biomedical Circuits and Systems (TBCAS)*, vol. 7, no. 3, pp. 363–375, Jun. 2013.

[22] E. A. Pelaez and E. R. Villegas, "LED power reduction trade-offs for ambulatory pulse oximetry," in *29th Annual International Conference of the IEEE Engineering in Medicine and Biology Society (EMBC)*, Aug. 2007, pp. 2296–2299.

[23] K. N. Glaros and E. M. Drakakis, "Trade-offs for low power integrated pulse oximeters," in *IEEE Biomedical Circuits and Systems Conference (BioCAS)*, Nov. 2009, pp. 245–248.

[24] D. L. Donoho, "Compressed sensing," *IEEE Transactions on Information Theory*, vol. 52, no. 4, pp. 1289–1306, Apr. 2006.

[25] E. J. Candés and M. B. Wakin, "An introduction to compressive sampling," *IEEE Signal Processing Magazine*, vol. 25, no. 2, pp. 21–30, Mar. 2008.

[26] P. K. Baheti and H. Garudadri, "An ultra low power pulse oximeter sensor based on compressed sensing," in *Sixth International Workshop on Wearable and Implantable Body Sensor Networks (BSN)*, Jun. 2009, pp. 144–148.

[27] V. R. Pamula *et al.*, "Computationally-efficient compressive sampling for low-power pulseoximeter system," in *Proceedings of 2014 IEEE Biomedical Circuits and Systems (BioCAS)*, Oct. 2014, pp. 69–72.

[28] V. R. Pamula *et al.*, "A 172 µW compressive sampling photoplethysmographic readout with embedded direct heart-rate and variability extraction from compressively sampled data," in *IEEE International Solid-State Circuits Conference (ISSCC)*, Jan. 2016, pp. 386–387.

[29] I. F. Gorodnitsky and B. D. Rao, "Sparse signal reconstruction from limited data using FOCUSS: A re-weighted minimum norm algorithm," *IEEE Transactions on Signal Processing*, vol. 45, no. 3, pp. 600–616, Mar. 1997.

[30] Z. Zhang, Z. Pi, and B. Liu, "TROIKA: A general framework for heart rate monitoring using wrist-type photoplethysmographic signals during intensive physical exercise," *IEEE Transactions on Biomedical Engineering (TBME)*, vol. 62, no. 2, pp. 522–531, Feb. 2015.

[31] P. Ahmmed *et al.*, "A wearable wrist-band with compressive sensing based ultra-low power photoplethysmography readout circuit," in *IEEE 16th International Conference on Wearable and Implantable Body Sensor Networks (BSN)*, May 2019, pp. 1–4.

[32] J. Dieffenderfer *et al.*, "Low-power wearable systems for continuous monitoring of environment and health for chronic respiratory disease," *IEEE Journal of Biomedical and Health Informatics (JBHI)*, vol. 20, no. 5, pp. 1251–1264, Sep. 2016.

[33] J. Lee *et al.*, "Comparison between red, green and blue light reflection photoplethysmography for heart rate monitoring during motion," in *35th Annual International Conference of the IEEE Engineering in Medicine and Biology Society (EMBC)*, Jul. 2013, pp. 1724–1727.

[34] L. Davies and U. Gather, "The identification of multiple outliers," *Journal of the American Statistical Association*, vol. 88, no. 423, pp. 782–792, 1993.

[35] N. R. Lomb, "Least-squares frequency analysis of unequally spaced data," *Astrophysics and Space Science*, vol. 39, no. 2, pp. 447–462, Feb. 1976.

[36] J. D. Scargle, "Studies in astronomical time series analysis. II - statistical aspects of spectral analysis of unevenly spaced data," *Astrophysical Journal*, vol. 263, no. 2, pp. 835–853, Dec. 1982.

[37] D. Biswas *et al.*, "Heart rate estimation from wrist-worn photoplethysmography: A review," *IEEE Sensors Journal*, vol. 19, no. 16, pp. 6560–6570, 2019.

[38] V. R. Pamula, C. Van Hoof, and M. Verhelst, "An ultra-low power, robust photoplethysmographic readout exploiting compressive sampling, artifact reduction, and sensor fusion," in *Hybrid ADCs, Smart Sensors for the IoT, and Sub-1V & Advanced Node Analog Circuit Design: Advances in Analog Circuit Design 2017*, P. Harpe, K. A. A. Makinwa, and A. Baschirotto, Eds. Cham, Switzerland: Springer International Publishing, 2018, pp. 145–163.

[39] A. Shcherbina *et al.*, "Accuracy in wrist-worn, sensor-based measurements of heart rate and energy expenditure in a diverse cohort," *Journal of Personalized Medicine*, vol. 7, no. 2, 2017, Article no. 3.

[40] D. G. Altman and J. M. Bland, "Measurement in medicine: The analysis of method comparison studies," *Journal of the Royal Statistical Society. Series D (The Statistician)*, vol. 32, no. 3, pp. 307–317, 1983.

[41] W. H. Press and G. B. Rybicki, "Fast algorithm for spectral analysis of unevenly sampled data," *Astrophysical Journal, Part 1*, vol. 338, pp. 277–280, Mar. 1989.

Authorized licensed use limited to: N.C. State University Libraries - Acquisitions & Discovery S. Downloaded on December 18,2024 at 21:30:29 UTC from IEEE Xplore. Restrictions apply.
© 2024 IEEE. Personal use is permitted, but republication/redistribution requires IEEE permission. See https://www.ieee.org/publications/rights/index.html for more information.